ACSNANO
www.acsnano.org
ARTICLE

DNA Nanostructures-Mediated Molecular Imprinting Lithography

Cheng Tian,[†,⊥] Hyojeong Kim,[†,⊥] Wei Sun,[‡,§] Yunah Kim,[†] Peng Yin,[‡,§] and Haitao Liu*[,†]

[†]Department of Chemistry, University of Pittsburgh, Pittsburgh, Pennsylvania 15260, United States
[‡]Wyss Institute for Biologically Inspired Engineering, Harvard University, Boston, Massachusetts 02115, United States
[§]Department of Systems Biology, Harvard Medical School, Boston, Massachusetts 02115, United States

Supporting Information

ABSTRACT: This paper describes the fabrication of polymer stamps using DNA nanostructure templates. This process creates stamps having diverse nanoscale features with dimensions ranging from several tens of nanometers to micrometers. DNA nanostructures including DNA nanotubes, stretched λ-DNA, two-dimensional (2D) DNA brick crystals with three-dimensional (3D) features, hexagonal DNA 2D arrays, and triangular DNA origami were used as master templates to transfer patterns to poly(methyl methacrylate) and poly(L-lactic acid) with high fidelity. The resulting polymer stamps were used as molds to transfer the pattern to acryloxy perfluoropolyether polymer. This work establishes an approach to using self-assembled DNA templates for applications in soft lithography.

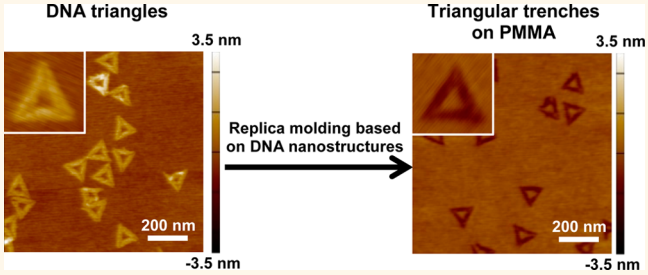

KEYWORDS: *pattern transfer, DNA nanostructures, polymer stamp, replica molding, nanoimprint lithography, nanofabrication, self-assembly*

Soft lithography uses a stamp to transfer micro- and nanoscale patterns.[1−5] The stamp is usually fabricated by casting a liquid precursor onto a master template with patterned structures. Soft lithography has been well developed and widely used for nanofabrication due to its simplicity, low cost, and compatibility with a wide range of substrates, especially soft materials and nonplanar surfaces.[2,5,6] The application of soft lithography, however, is fundamentally limited by the spatial resolution and diversity of the structures on the stamp.

Significant efforts have been put into the preparation of master templates, from which the stamp is derived.[5,7] Conventional lithography methods, such as photolithography and electron-beam (e-beam) lithography, are the most general approach to fabricating master templates. One-step 193 nm photolithography is widely used; however, it is not suitable for the fabrication of nanostructures with spacing less than 40 nm due to its diffraction-limited resolution. Although e-beam lithography can provide sub-10 nm resolution, the massive production of the master template is hindered by the high cost of this method.[8−10] In addition to the conventional lithographic methods, dip-pen nanolithography,[11] indentation lithography,[12] nanosphere lithography,[13] and block copolymer lithography[14−17] have been applied to offer nanoscale and even sub-10 nm features. Other relief structures such as crystallographic steps,[18] cracks,[19] and single-walled carbon nanotubes[20] have also been used to provide features with subnanometer or molecular-scale resolution. However, it still remains a challenge to develop a general method of constructing master templates and stamps with diverse nanoscale features and high spatial resolution.

In recent years, programmable DNA self-assembly[21−23] has produced a wide range of one-dimensional (1D),[24−27] two-dimensional (2D),[28−33] and three-dimensional (3D)[34−39] nanostructures with diverse and complex features. Assembled DNA nanostructures can be rationally designed and reliably synthesized. The assembly process is fast and easily implemented.[40] Thus, self-assembled DNA nanostructures can be used as nanofabrication templates due to ease of controlling their shapes with nanometer-scale spatial resolution. Along this direction, many approaches have been developed to transfer the pattern of DNA nanostructures to a wide range of materials. We briefly review these efforts below.

DNA nanostructures have been employed as masks to transfer the pattern to evaporated noble metal films.[41] Metalization has also been achieved through wet chemistry, and the resulting metal nanostructures have been used to pattern graphene.[42] By exploiting the difference in adsorption of water between DNA nanostructures and a SiO_2 substrate, DNA nanostructures have been used to modulate the rate of

Received: July 18, 2016
Accepted: January 4, 2017
Published: January 4, 2017

DOI: 10.1021/acsnano.6b04777
ACS Nano 2017, 11, 227−238

HF vapor phase etching to achieve pattern transfer to the SiO_2 substrate.[43] Based on the same principle, adsorption of water could control the rate of chemical vapor deposition of SiO_2 and TiO_2 on the DNA nanostructures and substrate to convert the pattern of DNA nanostructures into that of inorganic oxides.[44] Moreover, Al_2O_3-protected DNA nanostructures can be converted to carbon nanostructures by thermal annealing.[45] In addition to the 2D pattern transfer, 3D DNA nanostructures have served as molds to synthesize inorganic nanostructures with prescribed 3D shapes.[46]

DNA nanostructures are promising templates for materials science due to their structural complexity and diversity in the nanoscale. However, nanofabrication based on DNA nanostructures still faces several formidable challenges. First of all, the high cost of synthetic DNA hinders its application as a master template for large-scale patterning.[47] Second, there is a lack of reliable and faithful pattern transfer method that is compatible with existing fabrication processes due to the low mechanical and chemical stability of DNA nanostructures. Third, deterministic deposition of DNA nanostructures, which is critical to large-area fabrication, is still in its infancy. Existing approaches to controlling the deposition of DNA nanostructures suffer from low fidelity and high error rate.[48−51]

A strategy to partially overcome these problems is to establish a method to transfer complex DNA patterns to a polymer substrate. The resulting polymer stamps can be used as templates for the following patterning process, which reduces the cost, simplifies the fabrication process, and potentially overcomes the difficulties of scalable patterning. Recently, a linear DNA bundle with an average height of *ca.* 90 nm and an average width of *ca.* 879 nm was employed as a master template for the fabrication of a negative replica on an unsaturated polyester resin, which was further used to pattern a polyacrylamide gel.[52] However, the lateral dimension of the DNA bundle is relatively large (*ca.* 1 μm). To the best of our knowledge, none of the nanoscale DNA structures have been used as templates to fabricate polymer stamps with high diversity, complexity, and fidelity.

Herein we demonstrate an approach to using DNA nanostructures as master templates in a direct pattern transfer from DNA to polymers with high fidelity. The nanoscale features of the polymer can be rationally controlled by the design of the DNA nanostructures. A variety of DNA nanostructures were used to pattern poly(methyl methacrylate) (PMMA) and poly(L-lactic acid) (PLLA), including DNA nanotubes, 1D λ-DNA, 2D DNA brick crystals with 3D features, hexagonal DNA 2D arrays, and triangular DNA origami. The resulting polymer stamp could serve as a mold to transfer the pattern to an acryloxy perfluoropolyether (a-PFPE) polymer substrate.

RESULTS AND DISCUSSION

The fabrication of polymer stamps consists of six steps, as shown in Figure 1.[53] A silicon wafer with native oxide was cleaned by piranha solution and served as the substrate for DNA deposition (Figure 1a,b). After the DNA nanostructure was deposited, a polymer film (*e.g.*, PMMA) was spin-coated on the substrate to cover the DNA (Figure 1b,c). A negative replica formed on the subsurface of the film that was in contact with the DNA. Four edges of the film were scratched to expose the underlying silicon substrate (Figure 1c,d). Then a polydimethylsiloxane (PDMS) film was adhered to the polymer film as a flexible backing to assist in removing the polymer film

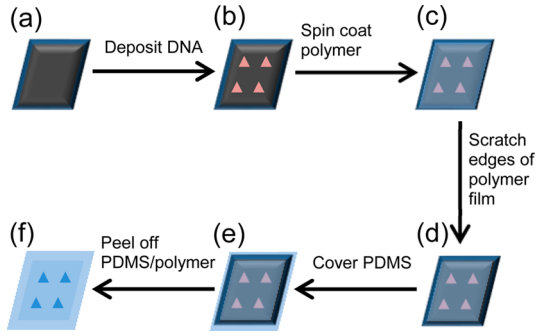

Figure 1. Fabrication of polymer stamps using DNA nanostructures as master templates. (a) The silicon wafer. (b) DNA nanostructures are on the silicon wafer. (c) A polymer film (*e.g.*, PMMA) is spin-coated on the silicon wafer. (d) Polymer film (*ca.* 1 mm wide) is removed from the four edges. (e) A PDMS film adheres to the polymer film as a flexible backing. (f) Drops of water are added to one edge of the exposed silicon wafer, and the PDMS/polymer film is peeled off.

from the silicon substrate in the next step (Figure 1d,e). Drops of water were added to one edge of the exposed silicon substrate and were allowed to penetrate into the interface between the hydrophobic polymer and the hydrophilic silicon wafer. In the last step, the PDMS/polymer film was peeled off and gently dried by a nitrogen stream (Figure 1e,f). The whole process can be completed in several minutes.

We first demonstrate the stamp fabrication using self-assembled DNA nanotubes that have a length of up to 60 μm and a width in the range of 30−70 nm.[25] The topography of the DNA master templates and polymer stamps was characterized by atomic force microscopy (AFM). In the AFM images, the height of the DNA nanotubes was measured to be 4.0 ± 0.5 nm. This small height is expected due to the collapse of the DNA nanotubes during the drying process (Figures 2a and S1a). Bundling of DNA nanotubes, however, was evident in some areas. After the polymer film was peeled off, the trenches corresponding to the DNA nanotubes were observed on the PMMA stamp. The 1D trenches were 3.2 ± 0.7 nm in depth, in good agreement with the height of the DNA nanotube master templates (Figures 2b and S1b). The measured width of the nanotube master template (67.1 ± 5.3 nm) was larger than the expected value, and the measured width of the 1D trenches on the PMMA stamps (39.7 ± 5.1 nm) was smaller than the expected value. We attribute this observation to the AFM probe convolution effect and the removal of the salt residues during the fabrication of the PMMA stamp. The bundling of DNA nanotubes produced wider and deeper 1D trenches. These results confirm a successful replication process from the DNA nanotubes to the PMMA stamp.

A similar stamp fabrication method was reported to replicate the pattern of single-walled carbon nanotubes (SWNTs) to high-modulus (~10 MPa) PDMS.[20] In that method, SWNTs attach to the silicon wafer through van der Waals interaction. In addition, an antiadhesion silane layer has to be deposited on the wafer to reduce the adhesion of PDMS to the silicon wafer. In our method, however, DNA nanostructures and the silicon wafer are bound through Mg^{2+}, *via* a likely much stronger electrostatic interaction. In addition, water can easily separate the hydrophilic silicon wafer from the hydrophobic polymer stamp, and the antiadhesion silane layer is not required. Most

DOI: 10.1021/acsnano.6b04777
ACS Nano 2017, 11, 227−238

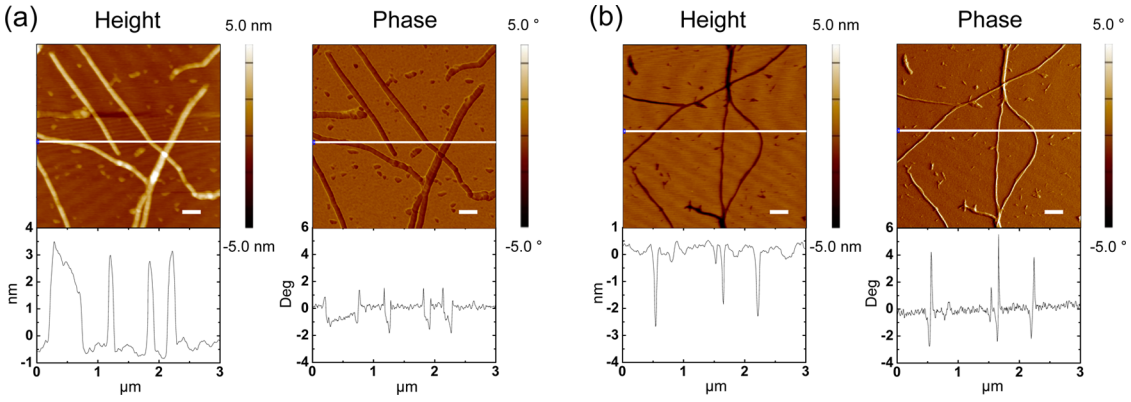

Figure 2. Fabrication of PMMA stamps by replication over DNA nanotubes. AFM height (left) and phase (right) images of (a) DNA nanotubes deposited on the silicon wafer and (b) the replica of nanotube patterns on PMMA stamps (top). Corresponding cross sections are shown at the bottom. Scale bars represent 300 nm.

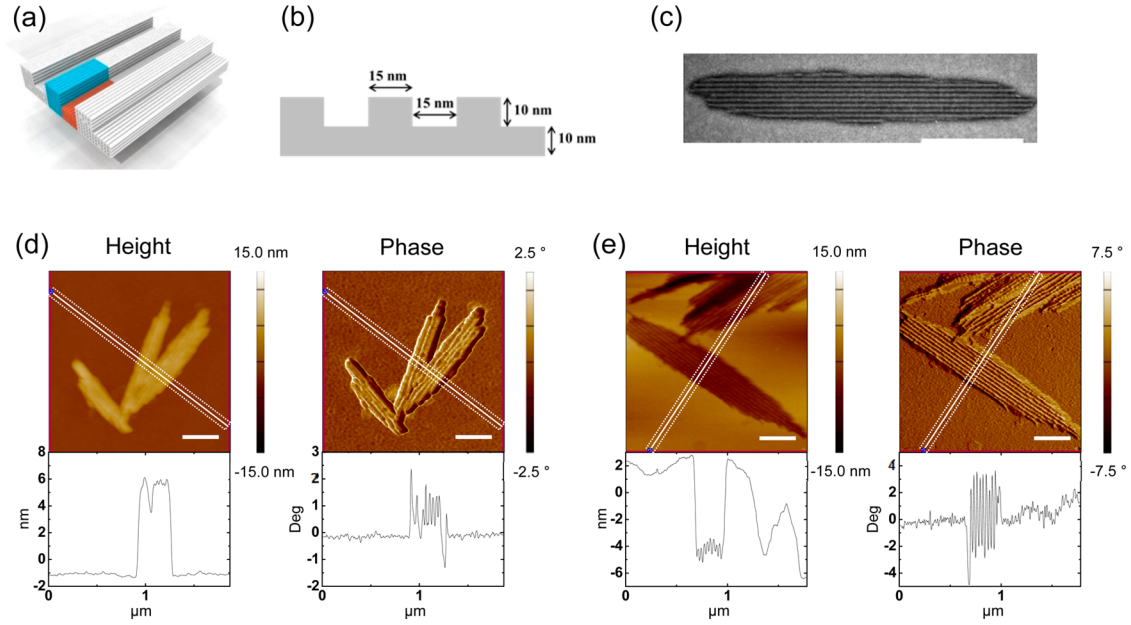

Figure 3. Fabrication of PMMA stamps by replication over 2D DNA brick crystals. (a) A model of 2D DNA brick crystal. The repeating unit is labeled as the blue and orange block. (b) Cross-section view of the model of the 2D DNA brick crystal. (c) Transmission electron microscopy (TEM) image of the 2D DNA brick crystal. The scale bar represents 500 nm. (d) AFM height (left) and phase (right) images of 2D DNA brick crystals deposited on a silicon wafer (top) and the corresponding cross sections (bottom). (e) AFM height (left) and phase (right) images of the replica of 2D DNA brick crystals on PMMA stamps (top) and the corresponding cross sections (bottom). Scale bars in d and e represent 300 nm.

importantly, our method can produce diverse nanostructures instead of simple linear trenches (see below).

Besides 1D nanostructures, 2D DNA brick crystals with defined 3D features could also serve as master templates to transfer 3D patterns to PMMA. Such 2D DNA brick crystals were prepared through the recently developed "DNA bricks" approach.[54] After a one-pot annealing process, 2D DNA brick crystals with parallel channels were assembled (Figure 3a). The channels are designed to be 10 nm high and 15 nm wide and are separated by ridges with a height of 10 nm and a width of 15 nm (Figure 3b), assuming 2.5 nm diameter per hydrated DNA helix.[54] The assembled brick crystals were imaged by transmission electron microscopy (TEM). The parallel channels were clearly visible in the TEM image, and the measured pitch of the brick crystal was 24.9 ± 0.5 nm, smaller than the theoretical value of 30 nm (Figure 3c). The decreased pitch of the 2D brick crystals is attributed to the staining and dehydration of the DNA brick crystals during TEM sample preparation and imaging in a vacuum. The AFM images show a consistent shape of the 2D brick crystals (Figures 3d and S2a,b). The height of the 2D brick crystals in the AFM image was 7.3 ± 0.3 nm, which is much smaller than the theoretical value of 20 nm, and the pitch was 29.9 ± 1.8 nm (expected value: 30 nm). The trenches within the DNA brick crystal were clearly visible in the AFM phase image; however, their full depth was not resolved in the topography image, likely due to the tip convolution effect. In addition, a high concentration of magnesium ions (40 mM) had to be used to stabilize the DNA brick crystals, resulting in their aggregation (Figures 3d,e and S2).

After the replication process, the negative replica of the DNA brick crystal could be clearly seen on the PMMA film (Figures

DOI: 10.1021/acsnano.6b04777
ACS Nano 2017, 11, 227−238

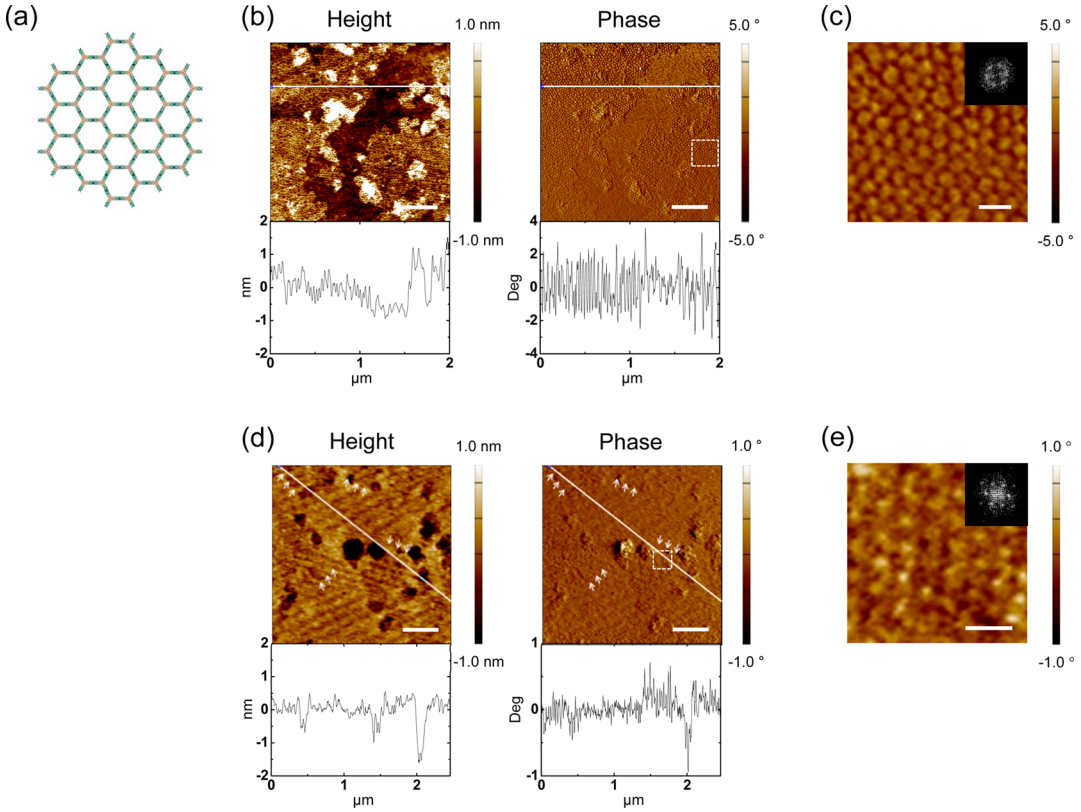

Figure 4. Fabrication of PMMA stamps by replication over hexagonal DNA 2D arrays. (a) Scheme of hexagonal DNA 2D arrays assembled from 3-point-star motifs. (b) AFM height (left) and phase (right) images of DNA 2D arrays assembled on the silicon wafer (top) and the corresponding cross sections (bottom). (c) Zoom-in view of the area in the white dashed box in b. The inset is the Fourier transform pattern of the image in c. (d) AFM height (left) and phase (right) images of the PMMA stamps (top) and the corresponding cross sections (bottom). (e) Zoom-in view of the area in the white dashed box in d. The inset is the Fourier transform pattern of the image in e. White arrows indicate the replicated patterns on PMMA. Scale bars in b and d represent 400 nm, and scale bars in c and e represent 50 nm.

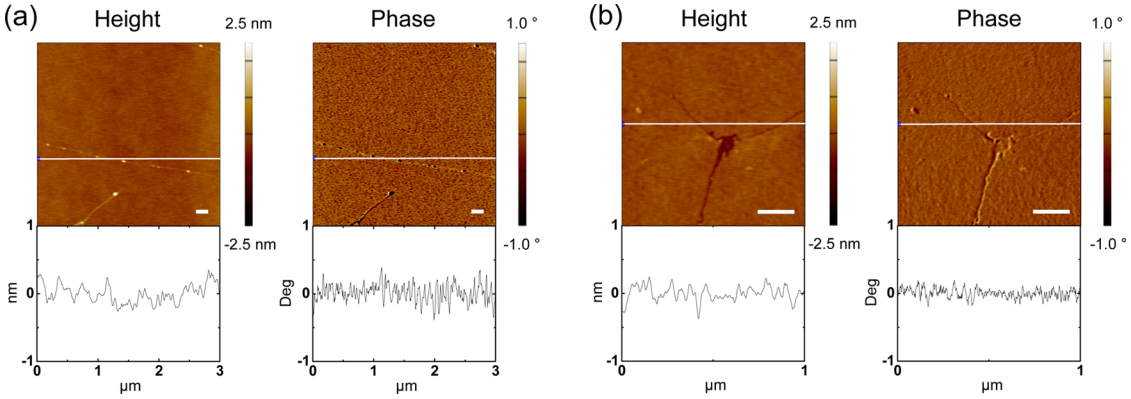

Figure 5. Fabrication of PMMA stamps by replication over the λ-DNA. AFM height (left) and phase (right) images of (a) λ-DNA deposited on the silicon wafer and (b) the replica of λ-DNA patterns on PMMA stamps. Corresponding cross sections are shown at the bottom. Scale bars represent 200 nm.

3e and S2c–e). The depth of the negative replica pattern was 7.7 ± 0.3 nm, in good agreement with that of the original 2D brick crystal (7.3 ± 0.3 nm) on the silicon wafer (Figure 3e). The trenches within the negative replica were clearly visible in the phase image, and the pitch was 30.3 ± 0.6 nm, which is close to that of the DNA master template (Figure 3e). Although the trenches were clearly visible in the topography image, their depth was not fully resolved and is much smaller than the expected value of 10 nm. This observation is similar to that of the DNA brick crystals. Nevertheless, the consistency of the shape, height, and pitch between 2D DNA brick crystals and their replica on PMMA stamps indicates a faithful replication process.

In addition to the DNA nanotubes and the 2D DNA brick crystals, DNA nanostructures with smaller feature sizes could also be used as master templates in our method. A hexagonal DNA 2D array was tested as a master template for the pattern transfer. The hexagonal DNA 2D array was self-assembled from DNA 3-point-star motifs (Figure 4a).[29] Each edge of the motif consists of two DNA double strands with a length of 4.5 turns.

DOI: 10.1021/acsnano.6b04777
ACS Nano 2017, 11, 227–238

To increase the surface coverage of the DNA 2D arrays, silicon-substrate-mediated annealing was used to directly grow the DNA 2D arrays on the silicon wafer.[55,56] A freshly cleaned silicon wafer was immersed in the DNA solution and annealed with DNA strands from 95 to 23 °C in 1 day. During this process, DNA motifs were adsorbed and confined to the SiO_2 surface to facilitate the self-assembly.[27] Figures 4b and S3a show that after the annealing most areas of the silicon wafer were covered by a monolayer of DNA 2D arrays with a hexagonal shape. The Fourier transform of the AFM phase image shows the expected 6-fold symmetry of the DNA array (Figure 4c). Big white spots were also observed, which we attribute to DNA aggregates and salt residues attached to the monolayer DNA. The section analysis shows that the repeating distance of the DNA 2D array was 29.7 ± 0.7 nm, in good agreement with the theoretical value of 30.3 nm.[29] On the surface of PMMA, the negative replica of the DNA 2D array appeared as an array of pillars and was highlighted by the white arrows in Figures 4d and S3c,d. The Fourier transform of the pattern shows 6-fold symmetry, which is consistent with the pattern of the DNA master template (Figure 4e). The periodicity of the pattern was measured by the averaged distance between adjacent pillars and found to be 29.7 ± 0.9 nm, almost identical to that of the DNA master template. The pillar-like PMMA pattern of the same symmetry and periodicity confirms the pattern replication from DNA 2D arrays to PMMA stamps.

To probe the resolution limit of this method, the feature size of the DNA nanostructures is further decreased to an individual DNA double helix. λ-DNA, a double-stranded phage DNA with a length of *ca.* 16 μm, was employed as a master template. The height and width (fwhm) of the individual λ-DNA were measured to be 0.3 ± 0.1 nm and 14.7 ± 3.2 nm, respectively (Figures 5a and S4a,b), although bundling of the λ-DNA was observed as well. After the replication, narrow 1D trenches with a depth of 0.4 ± 0.1 nm and a width (fwhm) of 11.1 ± 1.7 nm were observed on the PMMA stamp (Figures 5b and S4c–e), which represent the negative replica of the individual λ-DNA. This result suggests that even a single DNA double strand of a diameter of 2 nm might serve as a master template for the pattern transfer, suggesting the possibility of applying this method to pattern molecular-scale features.

All of the nanostructures tested above are either 1D linear structures or 2D nanostructures with periodic patterns. To increase the complexity of the patterns on the stamp, triangular DNA origami nanostructures[30,49] were employed as master templates for the pattern transfer. The triangular DNA origami is composed of a single layer of DNA double strands with a theoretical height of 2 nm and contains three trapezoidal domains. The edges of the adjacent trapezoidal domains are connected by the bridging staple strands, forming three small triangular holes at each vertex and one large triangular hole in the center (Figure 6a). According to the design, the inner length (the length of the sides of the central triangular hole), outer length, and full width at half-maximum (fwhm) of the trapezoidal sides of the DNA triangles are 55.0, 129.6, and 27.0 nm, respectively. AFM images show that the DNA triangles were randomly distributed on the silicon wafer and the central, large triangular holes were clearly visible (Figures 6b and S5a,b). Because of the resolution limitation of the AFM images, the bridging staple strands between the trapezoidal domains were not visible. As a result, the three smaller triangular holes at the vertex were shown as a linear gap. The tangling loop was

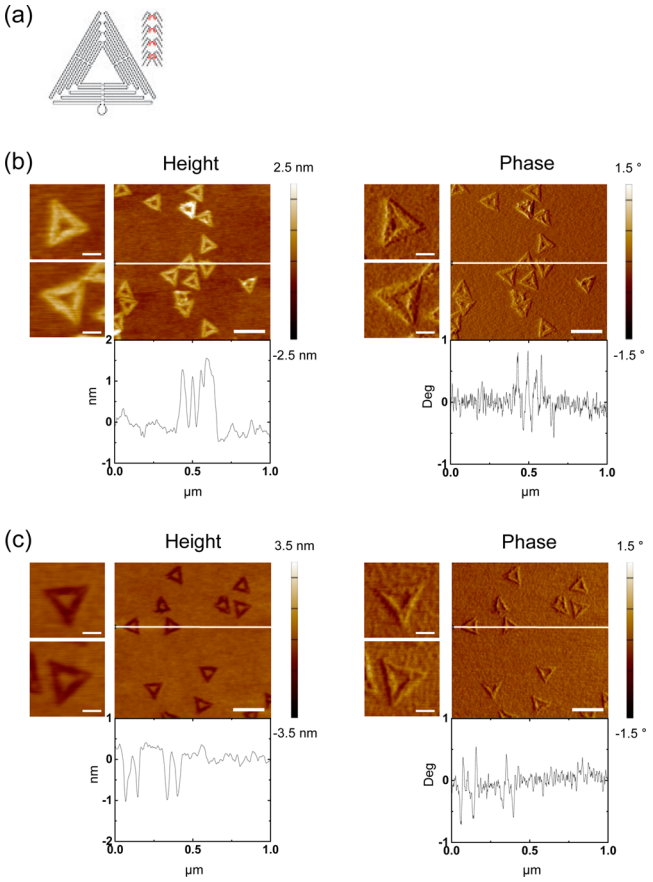

Figure 6. Fabrication of PMMA stamps by replication over the triangular DNA origami. (a) Folding path of the DNA scaffold strand in the DNA triangle. Red lines represent staple strands bridging the trapezoidal sides. Reprinted by permission from Macmillan Publishers Ltd.: *Nature* (ref 30), copyright 2006. (b) AFM height (left) and phase (right) images of the DNA triangles deposited on a silicon wafer (top) and the corresponding cross sections (bottom). (c) AFM height (left) and phase (right) images of triangular patterns on PMMA stamps (top) and the corresponding cross sections (bottom). Zoomed-in images are on the left of the corresponding images. Scale bars represent 200 nm (zoomed-out images) or 50 nm (zoomed-in images).

visible in some DNA triangles; in other structures, the tangling loops might have attached on top of the DNA triangle or beneath the structure so that they were not visible (Figure S6a). According to the AFM cross-section analysis, the height, inner length, outer length, and width (fwhm) of the trapezoidal sides of the DNA triangles were 1.6 ± 0.1 nm, 45.6 ± 2.0 nm, 131.2 ± 5.4 nm, and 38.0 ± 3.1 nm, respectively. The measured height of DNA nanostructures in AFM images might vary due to the differences in the probe–substrate and probe–sample interactions.[57] Due to the AFM probe convolution, the measured outer length and side width of DNA triangles increased compared with the theoretical value, and the measured inner length of DNA triangles was smaller than the theoretical value.

After the pattern transfer, triangular trenches appeared on the PMMA film, resembling the shape of the DNA origami (Figures 6c and S5c,d). Even the pattern of the tangling loop had been transferred to the PMMA stamp (Figure S6b). The averaged depth, inner length, outer length, and width (fwhm) of the triangular trenches were 1.0 ± 0.2 nm, 54.3 ± 2.6 nm,

DOI: 10.1021/acsnano.6b04777
ACS Nano 2017, 11, 227–238

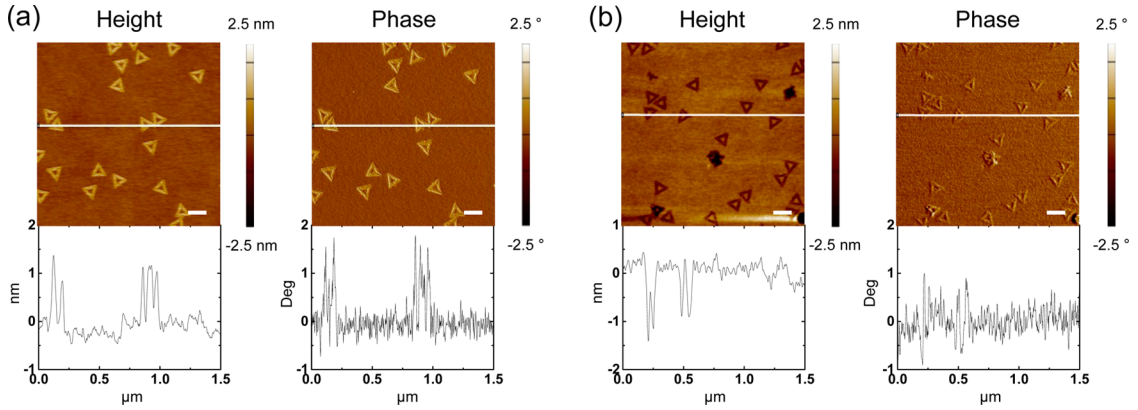

Figure 7. Fabrication of PLLA stamps by replication over the triangular DNA origami. (a) AFM height (left) and phase (right) images of DNA triangles deposited on a silicon wafer (top) and the corresponding cross sections (bottom). (b) AFM height (left) and phase (right) images of triangular patterns on the PLLA stamps (top) and the corresponding cross sections (bottom). Scale bars represent 150 nm.

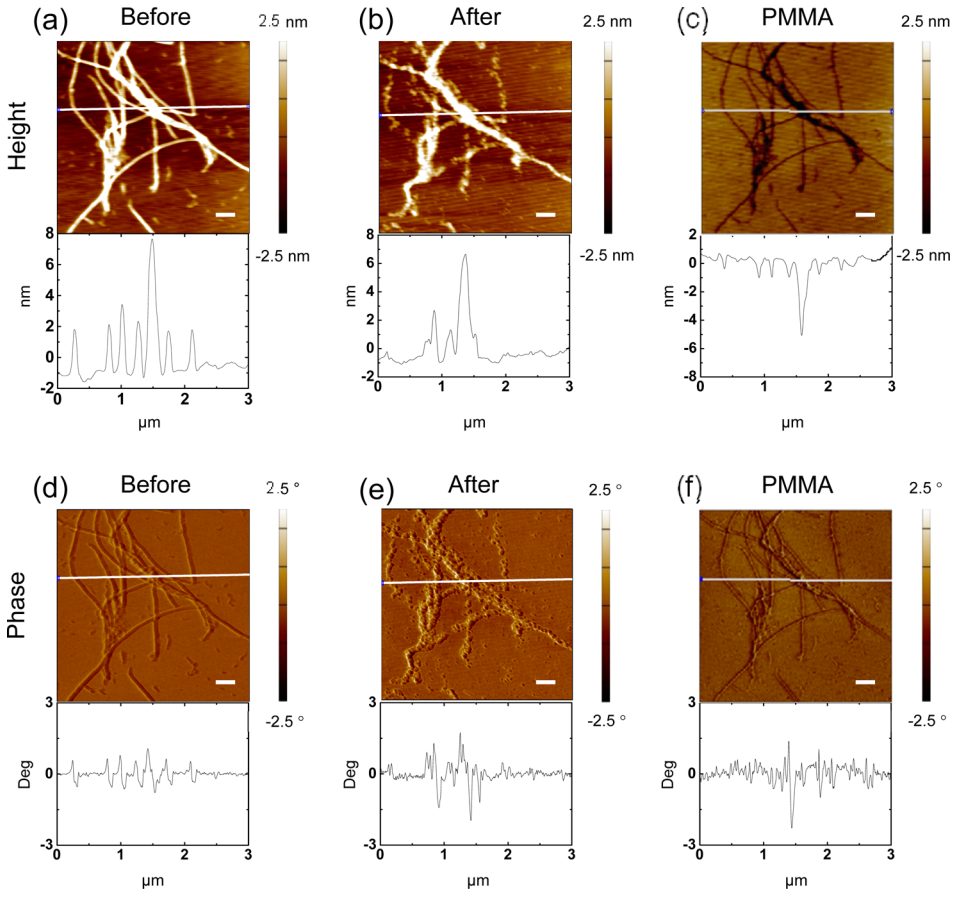

Figure 8. Comparison of features of the same location on the DNA master template and the polymer stamp. AFM height images and cross sections of DNA nanotubes deposited on a silicon wafer (a) before and (b) after the replication to PMMA stamps, and (c) PMMA replica of the same area. (d–f) Corresponding phase images and cross sections. Scale bars represent 300 nm. Note: images c and f were flipped horizontally to match the orientation of the DNA master template.

126.8 ± 3.8 nm, and 26.5 ± 3.1 nm, respectively. The decreased depth of the trenches is attributed to the removal of the salts during the pattern transfer. The inner length, outer length, and width of the triangular trenches are all consistent with the design. Similar to the DNA master templates, the small triangular holes did not show up on the PMMA stamps. Instead, we observed small bumps at the vertices of the triangular trenches, which is the replica of the gaps between the trapezoidal domains. This bump can be seen in the cross section of the vertices of the triangular trenches (Figure S7a–e). However, the height of the bump is much smaller than 1 nm, and in some trenches, the bump was not observed at all (Figure S7f). Both observations could be due to the mechanical instability of the bumps during the AFM imaging and/or inherent limitation of the pattern transfer. As the feature size of the DNA master template decreases, especially when nanometer-sized holes exist in the DNA master template, PMMA might not be able to fully fill the holes during the pattern

DOI: 10.1021/acsnano.6b04777
ACS Nano 2017, 11, 227–238

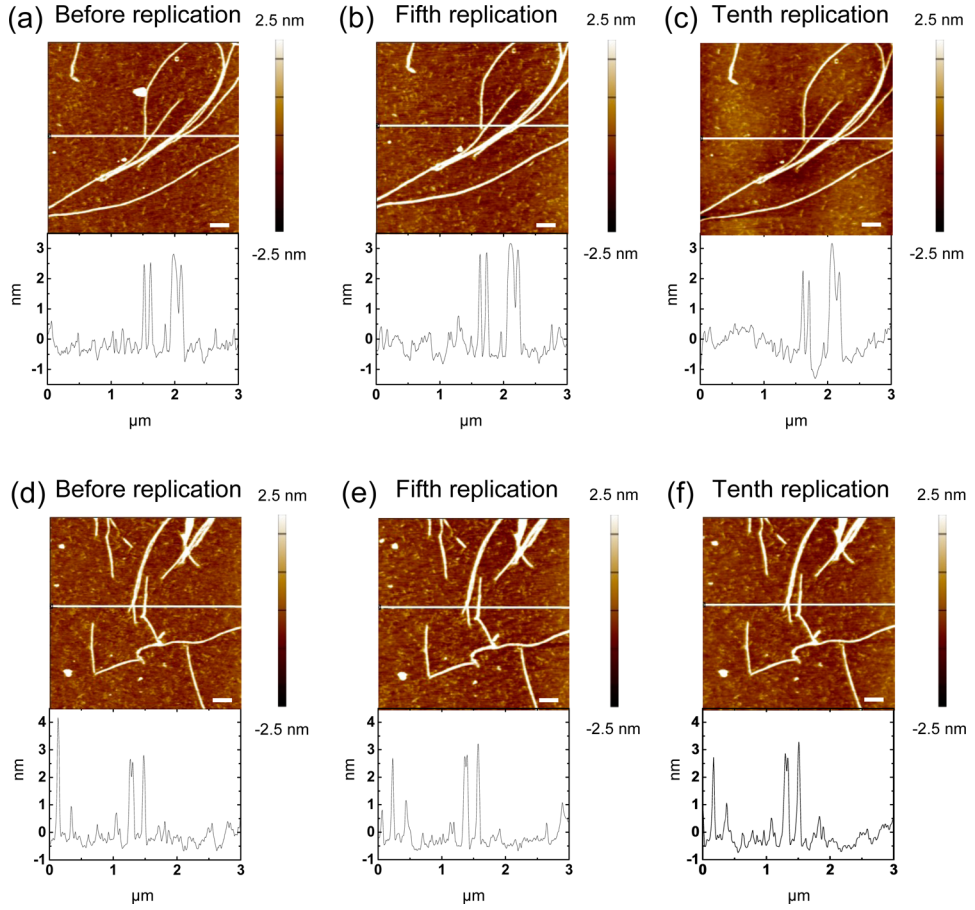

Figure 9. AFM height images of DNA nanotubes in two different locations (a, d) before the pattern transfer and after the (b, e) fifth and (c, f) 10th pattern transfer to the a-PFPE stamp (top). Corresponding cross sections are shown at the bottom. Scale bars represent 300 nm.

transfer, resulting in the decreased height and missing features in the PMMA replica. These results demonstrate that the overall features of the triangular DNA origami can be successfully transferred to the PMMA stamps with high fidelity, and the local features (*ca.* sub-5 nm) can be replicated to some extent.

Besides PMMA, other polymers such as PLLA could also be used as the stamp material in our method (Figures 7 and S8, 9). Both DNA triangles and DNA nanotubes could be precisely replicated to the PLLA stamps. Similar to the pattern transfer from DNA triangles to the PMMA stamp, the tangling loops and the gaps between the trapezoidal domains could also be transferred to the PLLA stamp (Figure S8). AFM cross sections indicate that the averaged depth and width (fwhm) of the triangular trenches on the PLLA stamps were 1.1 ± 0.2 nm and 27.1 ± 6.0 nm, respectively. The replication to the PLLA stamps offers a comparable resolution to that observed for the PMMA stamps, demonstrating the potential for replicating DNA nanostructure patterns into a wider range of polymers.

To evaluate the yield of the replication process and its impact on the DNA master template, we imaged the DNA master templates and the polymer stamps in the same location (Figures 8 and S10). Figure 8a and d show the topography and phase image of the DNA nanotubes on the silicon wafer, respectively. The corresponding negative replica on the polymer stamp (Figure 8c and f) matched well with the DNA master templates (Figure 8a and d), demonstrating a faithful pattern transfer. However, the nanotubes were partially damaged after the replication (Figure 8b and e), which we attribute to the water used to separate the master template and the stamp. To confirm the effect of water, we first used less water and decreased the incubation time (*i.e.*, the time between adding water to the silicon wafer and peeling off the polymer stamp). As a result, less DNA damage was observed (Figure S11). In addition, DNA nanotubes were also replicated to the a-PFPE polymer stamp, during which process water was not used. AFM height images in Figure S12 illustrate that the features and height of DNA nanotubes were preserved after the replication to the a-PFPE polymer, confirming that none of the DNA materials were transferred to the stamp. In addition, the AFM phase image also shows that the DNA nanostructure template was not trapped in the polymer stamps. Since the phase image is sensitive to the chemical composition, if DNA nanostructures were trapped in the trenches, the features would be visible in the phase image but not in the height image. Therefore, the yield of the pattern transfer can be assessed by examining the consistency between AFM height and phase images. In all the figures mentioned above, the position and shape of the features in the height and phase images matched with each other, suggesting the absence of trapped DNA nanostructures in the polymer stamps.

In addition to the high yield of replication, the DNA master templates can also be used in a repeated manner to transfer the pattern to the a-PFPE stamp. Figures 9 and S13 show the AFM images of the DNA master templates before the replication process and after the fifth and 10th replication. The features of

DOI: 10.1021/acsnano.6b04777
ACS Nano 2017, 11, 227–238

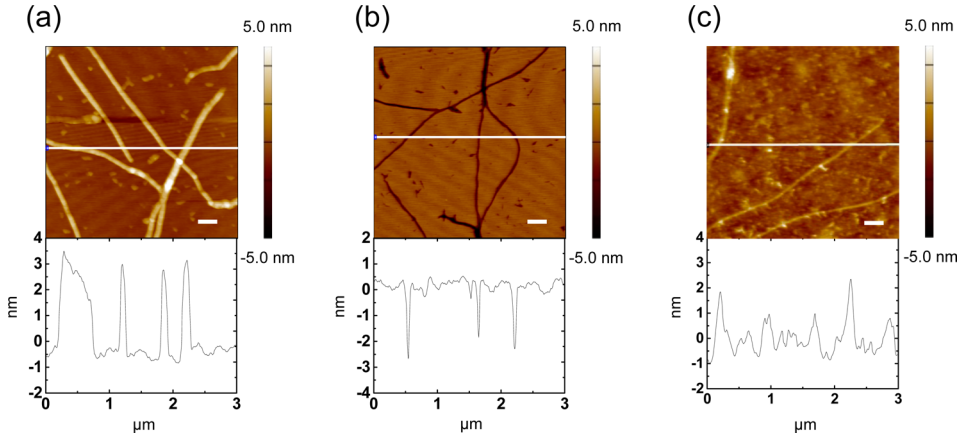

Figure 10. AFM height images of (a) DNA nanotubes on a silicon wafer, (b) DNA nanotube patterns on the PMMA stamp, and (c) DNA nanotube pattern on an a-PFPE substrate transferred from the PMMA stamp by the replica molding. Corresponding cross sections are shown at the bottom. Scale bars represent 300 nm. Note: a and b are also shown in Figure 2.

the DNA master templates were not damaged during the 10 times of replication. The repeated use of DNA master templates would greatly reduce the cost and facilitate its applications. We note that DNA master templates cannot be repeatedly used to transfer the pattern to PMMA or PLLA stamps at this stage because water, which is used to release the stamp, may damage the features of the DNA templates as mentioned above. To achieve the repeated use of the DNA master templates, polymers with low surface energy (*e.g.*, a-PFPE) should be employed to facilitate the separation of the stamp from the master template without the help of water. Alternatively, it is also possible to protect the DNA nanostructures using a nanometer-thin oxide coating (*e.g.*, Al_2O_3) grown by atomic layer deposition.[45]

The stability of the stamp is also crucial for their applications of soft lithography. To assess the stability of the features on PMMA, a DNA triangle-patterned PMMA film was imaged immediately after being peeled off and again after 10 days of aging in the air (Figure S14). As mentioned above, the depth and width (fwhm) of triangular trenches in the fresh PMMA film were 1.0 ± 0.2 nm and 26.5 ± 3.1 nm, respectively. After 10 days of aging in the air, section analysis in Figure S14b indicates that the triangular trenches were 0.9 ± 0.1 nm in depth and 27.8 ± 2.8 nm in width. The 10 days of aging in the air did not change the features on the PMMA film significantly. The PMMA stamps possess enough stability for long-term storage.

The resulting polymer stamp could serve as a mold to transfer the pattern to other materials. Figure 10 shows the replica molding of nanotube patterns on a PMMA stamp into a photocurable a-PFPE.[58] In this experiment, the a-PFPE prepolymer was spin-cast as a thin film on the PMMA stamps with the DNA nanotube relief and then cured under UV illumination. Due to the low surface energy of a-PFPE, the PMMA and a-PFPE films could be easily separated. A DNA nanotube pattern was observed on the a-PFPE film with a height of 2.5 ± 0.5 nm and a width of 41.6 ± 6.9 nm, demonstrating a faithful pattern transfer from PMMA stamps to the a-PFPE polymer film (Figures 10 and S15). Compared with the DNA nanotube master templates, both the depth/height and width of the patterns on the PMMA and a-PFPE were smaller. The average height/depth and width of DNA nanotube master templates, PMMA trenches, and nanotube patterns on the a-PFPE were 4.0 and 67.1 nm, 3.2 and 39.7 nm, and 2.5 and 41.6 nm, respectively. The exact reason for this decrease in dimensions is not clear at this stage. One possibility is that the removal of the salt residues during the fabrication of the PMMA stamp leads to the smaller size. We also note that a similar decrease in the feature size was previously reported on replicating a carbon nanotube pattern to the a-PFPE and then to the polyurethane.[58] In addition, the surface roughness of the a-PFPE film was measured to be 322.7 pm, which is much larger than that of the PMMA stamp (158.2 pm) but similar to that of the a-PFPE stamp (412.8 pm) that was produced from the DNA master templates and shown in Figure S12. High surface roughness of a-PFPE mold was also reported before,[58] suggesting that it is likely an intrinsic property of this material and not a result from the molding process. Besides the PMMA stamp, the PLLA stamp could also serve as a mold to transfer the pattern to the a-PFPE with comparable fidelity (Figure S16).

Finally, we investigated the repeated use of the polymer stamps for the application of replica molding. We found that the polymer stamp film often delaminated from the PDMS backing layer and broke during the separation of the stamp from the mold. We attribute this observation to the micrometer-scale thinness of the stamp and its low affinity to PDMS. Part of the polymer stamp film remained on the PDMS backing layer, from which we were able to verify that the nanoscale features there were not damaged after molding the a-PFPE film (Figure S17). Therefore, the polymer stamps should be reusable if an alternative molding process could be developed to protect the physical integrity of the polymer stamp. We note that others have reported the repeated use of polymer stamps, including PMMA, for replica molding and other nanoscale patterning applications.[59−67] Work is under way to fully explore the applications of the polymer stamps that we produced in this study.

CONCLUSIONS

We have demonstrated a general method of fabricating polymer stamps using DNA nanostructure master templates with high fidelity. DNA nanotubes, 1D λ-DNA, 2D DNA brick crystals with 3D features, hexagonal DNA 2D arrays, and triangular DNA origami have been tested as master templates to replicate their features to PMMA and PLLA. The resulting PMMA stamp has been applied as a mold to transfer the pattern to

DOI: 10.1021/acsnano.6b04777
ACS Nano 2017, 11, 227−238

photo-cross-linked a-PFPE. In addition to replica molding, the polymer stamp can be potentially used in many other applications, in particular contact printing of small molecules and proteins.[4,5,66,67] Since DNA master templates with diverse features can be rationally designed and constructed, our method could enable the fabrication of polymer stamps with varieties of nanoscale features, some of which (*e.g.*, alphabets) are inaccessible by other self-assembly methods. The integration of DNA nanotechnology with soft lithography offers alternative master templates and enriches the nanoscale features of polymer stamps to facilitate their applications.

To apply DNA nanostructures in the scalable nanofabrication, the limitation of large-area patterning in our method needs to be overcome. High-throughput nanopatterning is important for the nanofabrication and has been realized by e-beam lithography[9,10] and directed self-assembly of block copolymer.[15−17] However, the difficulties of controlling deposition of DNA nanostructures and defects in the self-assembled DNA nanostructures limit their applications in large-area patterning. Further studies are still needed to address these challenges. In addition, the technical issues associated with the repeated use of the polymer stamp in our method need to be overcome. At the current stage, this challenge could be compensated by generating multiple copies of the polymer stamps based on a DNA master template. Ways to increase the chemical and mechanical stability of the DNA master template (*e.g.*, by a conformal coating of an inorganic oxide film[44,45]) are being explored to further facilitate the scalable nanofabrication using this template.

MATERIALS AND METHODS

Materials. Silicon wafer (Si[110], with native oxide) was purchased from University Wafers. The scaffold strand M13mp18 for the triangular DNA origami and λ-DNA were purchased from Bayou Biolabs (Metairie, LA, USA) and New England Biolabs (Ipswich, MA, USA), respectively. Short staple strands for the triangular DNA origami and DNA strands for DNA nanotubes, 2D arrays, and 2D brick crystals were synthesized by Integrated DNA Technologies (Coralville, IA, USA). 2-Amino-2-(hydroxymethyl)-1,3-propanediol (Tris), ethylenediaminetetraacetic acid (EDTA), magnesium acetate tetrahydrate, sulfuric acid, hydrogen peroxide solution (30% H_2O_2), poly(methyl methacrylate), and poly(L-lactic acid) were purchased from Sigma-Aldrich (St. Louis, MO, USA). Acetic acid (glacial) and nickel chloride hexahydrate (ACS Certified) were purchased from Fisher Scientific (Fair Lawn, NJ, USA). Dichloromethane was purchased from Acros Organics (Fair Lawn, NJ, USA). Ethanol was purchased from Sigma-Aldrich and Decon Laboratories, Inc. (King of Prussia, PA, USA). PDMS film was prepared with Sylgard 184 silicone elastomer kit (Dow Corning, Midland, MI, USA). Fluorinated acrylate oligomer CN4002 (1400 g mol^{-1}) was purchased from Sartomer Americas (Exton, PA, USA), and the photoinitiator Irgacure 4265 was purchased from BASF (Florham Park, NJ, USA). All materials were used as received. The UV lamp (100 W, 365 nm) was purchased from Cole-Parmer (Vernon Hills, IL, USA). High-purity water (18.3 MΩ) was produced by a water purification system (Barnstead MicroPure Standard, Thermo Scientific, Waltham, MA, USA) and used throughout the entire experiment.

Preparation of the Silicon Wafer. The silicon wafer was cleaned by the hot piranha solution (7:3 concentrated H_2SO_4/30% H_2O_2). **Warning:** *Piranha solution presents an explosion danger and should be handled with extreme care; it is a strong oxidant and reacts violently with organic materials. All work should be performed in a fume hood. Wear proper protective equipment.*

Preparation and Deposition of DNA Nanotubes on a Silicon Wafer. The design of DNA nanotubes was previously reported.[25] The DNA single strand was diluted in TAE/Mg^{2+} buffer (125 mM Mg^{2+}) with a final concentration of 1 μM. The DNA solution was slowly cooled from 95 °C to 23 °C in 2 days. Nickel chloride solution (70 μL of 2 mM) was placed on a cleaned silicon wafer and immediately blown away with nitrogen gas. Annealed DNA nanotube solution was deposited on the pretreated silicon wafer and incubated in a humid chamber for 15 min. The sample was dried using nitrogen gas, immersed in ethanol/water (9:1) solution for 10 s to remove the salts, and then dried using nitrogen gas again.

Preparation and Deposition of DNA 2D Brick Crystals on a Silicon Wafer.[54] Unpurified DNA strands were mixed in an equimolar stoichiometric ratio in 0.5× Tris/EDTA buffer [Tris (5 mM, pH 8.0) and EDTA (1 mM)] supplemented with 40 mM $MgCl_2$. The final concentration of each strand was 200 nM. The DNA solution was annealed in a PCR thermo-cycler using a fast linear cooling step from 80 to 60 °C over 1 h and then from 60 to 25 °C over 72 h. DNA solution was diluted by 10 times in 0.5× Tris/EDTA buffer with 40 mM $MgCl_2$. The diluted DNA solution (10 μL) was deposited on the cleaned silicon wafer and incubated in a humid chamber for 15 min. The sample was dried using nitrogen gas, immersed in ethanol/water (9:1) solution for 5 s, and then dried using nitrogen gas again.

Preparation and Deposition of DNA Two-Dimensional Arrays Assembled from the 3-Point-Star Motif on a Silicon Wafer. The design of the DNA 2D array was previously reported.[29] To increase the surface coverage, DNA 2D arrays were directly assembled on the silicon wafer. Three DNA single strands were mixed in TAE/Mg^{2+} buffer at a concentration of 25 nM in terms of the 3-point-star motifs. The cleaned silicon wafer was immersed in 10× TAE/Mg^{2+} buffer [Tris (400 mM, pH 8.0), acetic acid (200 mM), EDTA (10 mM), and Mg $(CH_3COO)_2$ (125 mM)] for 3 h to increase the surface concentration of magnesium ions, which were used to bind DNA on the silicon wafer.[55] After 3 h of incubation, the silicon wafer was directly immersed into the prepared DNA solution. The DNA solution together with the silicon wafer was slowly cooled from 95 °C to 23 °C in 1 day. After the annealing, the silicon wafer was taken out of the DNA solution, immediately immersed in ethanol/water (7:3) solution for 5 s, and then dried using nitrogen gas.

Preparation and Deposition of λ-DNA on a Silicon Wafer. λ-DNA (500 μg/mL) was diluted in TAE/Mg^{2+} buffer by three times. Since λ-DNA was difficult to attach to the silicon wafer, nickel ions were used to provide an extra binding force between DNA and the silicon wafer. Nickel chloride solution (100 μL of 1 mM) was deposited on the cleaned silicon wafer for 10 s and immediately dried using nitrogen gas. Then 10 μL of diluted λ-DNA solution was deposited on the silicon wafer and incubated in a humid chamber for 15 min. The sample was dried using nitrogen gas, immersed in ethanol/water (9:1) solution for 5 s, and then dried using nitrogen gas again.

Preparation and Deposition of the Triangular DNA Origami on a Silicon Wafer. The design and assembly of the triangular DNA origami were previously reported.[30,49] M13mp18 (1.6 nM) was mixed with 253 short staple strands (16 nM) in TAE/Mg^{2+} buffer [Tris (40 mM, pH 8.0), acetic acid (20 mM), EDTA (1 mM), and Mg $(CH_3COO)_2$ (12.5 mM)]. The sample was cooled from 95 °C to 20 °C at the rate of 1 °C/min. After the annealing, 100 μL of DNA origami solution was purified by rinsing away excess staple strands using 400 μL of TAE/Mg^{2+} buffer in a 100 kDa MW centrifuge filter (Microcon YM-100, Millipore, Billerica, MA, USA) on a single-speed benchtop microcentrifuge (VWR Galaxy Ministar). The rinsing process was repeated another two times. The final volume of DNA origami solution was 100 μL, the same as before the purification. Purified triangular DNA origami solution (10 μL) was deposited on the cleaned silicon wafer and incubated in a humid chamber for 15 min. The sample was dried using nitrogen gas, immersed in ethanol/water (9:1) solution for 5 s to remove the salts, and then dried using nitrogen gas again.

Fabrication of PMMA and PLLA Stamps Using DNA Nanostructures as Master Templates. The fabrication of polymer stamps consists of five steps.[53] First, a PMMA or PLLA film was prepared by spin coating on a silicon wafer with DNA nanostructures

DOI: 10.1021/acsnano.6b04777
ACS Nano 2017, 11, 227−238

(3 wt % PMMA or PLLA dissolved in dichloromethane, 3000 rpm, 1 min). The spin coating was repeated three times to increase the film thickness. Second, four edges of the polymer film were scratched to remove *ca.* 1 mm width of the film to expose the underlying silicon substrate. Third, a PDMS film with a thickness of 1−2 mm was adhered to the polymer film as a flexible backing. Fourth, several drops of water were added to one edge of the exposed silicon substrate and were allowed to penetrate into the interface between the hydrophobic polymer and hydrophilic silicon wafer. Fifth, after several seconds, as the interface was fully filled with water, the PDMS/polymer film was immediately peeled off and gently dried using nitrogen gas.

Fabrication of a-PFPE Polymer Stamps Using DNA Nanostructures as Master Templates. a-PFPE prepolymer resin consisted of a fluorinated acrylate oligomer, CN 4002, and a photoinitiator, Irgacure 4265 (0.5 wt %). The prepolymer resin was mixed for at least 2 h using a Teflon magnetic stirrer on a stirring plate. This photocurable liquid resin was filtered through a 0.2 μm pore size syringe filter and spin-coated on the silicon wafer with DNA nanostructures at 4000 rpm for 30 s. On top of the spin-coated a-PFPE prepolymer film, the filtered a-PFPE liquid resin was pooled to make an a-PFPE film thick enough to be peeled off with a tweezer after curing. The a-PFPE prepolymer was cured with UV light (365 nm) for 2 h under nitrogen gas. The a-PFPE composite stamp was peeled off from the wafer with a tweezer.

Replica Molding of Patterns on the PMMA or PLLA Stamps into the a-PFPE Film. This process is similar to the one outlined above, except a PMMA or PLLA stamp was used in place of the DNA nanostructure template.

Atomic Force Microscopy Analysis. The imaging was performed by tapping-mode on an Asylum MFP-3D atomic force microscope with NSC15/Al BS, RTESPA-300, or SSS-FMR-SPL AFM probes in the air. The tip−surface interaction was minimized by optimizing the scan set-point. The NSC15/AL BS AFM probe (325 kHz, 40 N/m) was purchased from MikroMasch (Lady's Island, SC, USA). The RTESPA-300 AFM probe (300 kHz, 40 N/m) was purchased from Bruker (Camarillo, CA, USA). The SSS-FMR-SPL AFM probe (75 kHz, 2.8 N/m) was purchased from NanoAndMore USA (Watsonville, CA, USA) and was used for the high-resolution imaging of DNA triangles and triangular patterns on the PMMA and PLLA. The Fourier transform was carried out by ImageJ, an imaging processing software.[68]

Transmission Electron Microcopy. An annealed sample of DNA brick crystals (2.5 μL) was adsorbed on a glow-discharge-treated carbon-coated TEM grid for 2 min. The grid was then stained by a 2% aqueous uranyl formate solution containing 25 mM NaOH for 10 s. Imaging was performed using a JEOL JEM-1400 TEM operating at 80 kV.

ASSOCIATED CONTENT

Supporting Information

The Supporting Information is available free of charge on the ACS Publications website at DOI: 10.1021/acsnano.6b04777.

Additional figures (PDF)

AUTHOR INFORMATION

Corresponding Author

*E-mail: hliu@pitt.edu.

ORCID

Haitao Liu: 0000-0003-3628-5688

Author Contributions

⊥C. Tian and H. Kim contributed equally.

Notes

The authors declare no competing financial interest.

ACKNOWLEDGMENTS

H.L. thanks the support from ONR (N000141310575 and N000141512520) and the University of Pittsburgh CRDF fund. P.Y. acknowledges funding support from NSF (CMMI-1333215 and CMMI-1344915), ONR (N00014-14-1-0610), and AFOSR (MURI FATE, FA9550-15-1-0514).

REFERENCES

(1) Xia, Y. N.; Whitesides, G. M. Soft Lithography. *Annu. Rev. Mater. Sci.* **1998**, *28*, 153−184.

(2) Gates, B. D.; Xu, Q. B.; Stewart, M.; Ryan, D.; Willson, C. G.; Whitesides, G. M. New Approaches to Nanofabrication: Molding, Printing, and Other Techniques. *Chem. Rev.* **2005**, *105*, 1171−1196.

(3) Rogers, J. A.; Nuzzo, R. G. Recent Progress in Soft Lithography. *Mater. Today* **2005**, *8*, 50−56.

(4) Qin, D.; Xia, Y.; Whitesides, G. M. Soft Lithography for Micro- and Nanoscale Patterning. *Nat. Protoc.* **2010**, *5*, 491−502.

(5) Lipomi, D. J.; Martinez, R. V.; Cademartiri, L.; Whitesides, G. M. Soft Lithographic Approaches to Nanofabrication. In *Polymer Science: A Comprehensive Reference*; Matyjaszewski, K., Möller, M., Eds.; Elsevier Science: Oxford, 2012; pp 211−231.

(6) Lipomi, D. J.; Martinez, R. V.; Whitesides, G. M. Use of Thin Sectioning (Nanoskiving) to Fabricate Nanostructures for Electronic and Optical Applications. *Angew. Chem., Int. Ed.* **2011**, *50*, 8566−8583.

(7) Xia, Y. N.; Rogers, J. A.; Paul, K. E.; Whitesides, G. M. Unconventional Methods for Fabricating and Patterning Nanostructures. *Chem. Rev.* **1999**, *99*, 1823−1848.

(8) Pease, R. F.; Chou, S. Y. Lithography and Other Patterning Techniques for Future Electronics. *Proc. IEEE* **2008**, *96*, 248−270.

(9) Wieland, M. J.; de Boer, G.; ten Berge, G. F.; van Kervinck, M.; Jager, R.; Peijster, J. J. M.; Slot, E.; Steenbrink, S.; Teepen, T. F.; Kampherbeek, B. J. MAPPER: High Throughput Maskless Lithography. *Proc. SPIE* **2010**, 76370F.

(10) Lin, B. J. Future of Multiple-E-Beam Direct-Write Systems. *Proc. SPIE* **2012**, 832302.

(11) Shim, W.; Braunschweig, A. B.; Liao, X.; Chai, J.; Lim, J. K.; Zheng, G.; Mirkin, C. A. Hard-Tip, Soft-Spring Lithography. *Nature* **2011**, *469*, 516−521.

(12) Gong, J.; Lipomi, D. J.; Deng, J.; Nie, Z.; Chen, X.; Randall, N. X.; Nair, R.; Whitesides, G. M. Micro- and Nanopatterning of Inorganic and Polymeric Substrates by Indentation Lithography. *Nano Lett.* **2010**, *10*, 2702−2708.

(13) Haynes, C. L.; Van Duyne, R. P. Nanosphere Lithography: a Versatile Nanofabrication Tool for Studies of Size-Dependent Nanoparticle Optics. *J. Phys. Chem. B* **2001**, *105*, 5599−5611.

(14) Hawker, C. J.; Russell, T. P. Block Copolymer Lithography: Merging "Bottom-Up" with "Top-Down" Processes. *MRS Bull.* **2005**, *30*, 952−966.

(15) Stoykovich, M. P.; Muller, M.; Kim, S. O.; Solak, H. H.; Edwards, E. W.; de Pablo, J. J.; Nealey, P. F. Directed Assembly of Block Copolymer Blends into Nonregular Device-Oriented Structures. *Science* **2005**, *308*, 1442−1446.

(16) Ruiz, R.; Kang, H. M.; Detcheverry, F. A.; Dobisz, E.; Kercher, D. S.; Albrecht, T. R.; de Pablo, J. J.; Nealey, P. F. Density Multiplication and Improved Lithography by Directed Block Copolymer Assembly. *Science* **2008**, *321*, 936−939.

(17) Jeong, S. J.; Kim, J. Y.; Kim, B. H.; Moon, H. S.; Kim, S. O. Directed Self-Assembly of Block Copolymers for Next Generation Nanolithography. *Mater. Today* **2013**, *16*, 468−476.

(18) Elhadj, S.; Rioux, R. M.; Dickey, M. D.; DeYoreo, J. J.; Whitesides, G. M. Subnanometer Replica Molding of Molecular Steps on Ionic Crystals. *Nano Lett.* **2010**, *10*, 4140−4145.

(19) Xu, Q. B.; Mayers, B. T.; Lahav, M.; Vezenov, D. V.; Whitesides, G. M. Approaching Zero: Using Fractured Crystals in Metrology for Replica Molding. *J. Am. Chem. Soc.* **2005**, *127*, 854−855.

(20) Hua, F.; Sun, Y. G.; Gaur, A.; Meitl, M. A.; Bilhaut, L.; Rotkina, L.; Wang, J. F.; Geil, P.; Shim, M.; Rogers, J. A. Polymer Imprint

Lithography with Molecular-Scale Resolution. *Nano Lett.* **2004**, *4*, 2467−2471.
(21) Seeman, N. C. Nanomaterials Based on DNA. In *Annual Reviews of Biochemistry*; Kornberg, R. D., Raetz, C. R. H., Rothman, J. E., Thorner, J. W., Eds.; Annual Reviews: Palo Alto, 2010; pp 65−87.
(22) Lin, C. X.; Liu, Y.; Rinker, S.; Yan, H. DNA Tile Based Self-Assembly: Building Complex Nanoarchitectures. *ChemPhysChem* **2006**, *7*, 1641−1647.
(23) Aldaye, F. A.; Palmer, A. L.; Sleiman, H. F. Assembling Materials with DNA As the Guide. *Science* **2008**, *321*, 1795−1799.
(24) Rothemund, P. W. K.; Ekani-Nkodo, A.; Papadakis, N.; Kumar, A.; Fygenson, D. K.; Winfree, E. Design and Characterization of Programmable DNA Nanotubes. *J. Am. Chem. Soc.* **2004**, *126*, 16344−16352.
(25) Liu, H. P.; Chen, Y.; He, Y.; Ribbe, A. E.; Mao, C. D. Approaching the Limit: Can One DNA Oligonucleotide Assemble into Large Nanostructures? *Angew. Chem., Int. Ed.* **2006**, *45*, 1942−1945.
(26) Yin, P.; Hariadi, R. F.; Sahu, S.; Choi, H. M. T.; Park, S. H.; LaBean, T. H.; Reif, J. H. Programming DNA Tube Circumferences. *Science* **2008**, *321*, 824−826.
(27) Tian, C.; Zhang, C.; Li, X.; Hao, C.; Ye, S.; Mao, C. Approaching the Limit: Can One DNA Strand Assemble into Defined Nanostructures? *Langmuir* **2014**, *30*, 5859−5862.
(28) Ding, B. Q.; Sha, R. J.; Seeman, N. C. Pseudohexagonal 2D DNA Crystals from Double Crossover Cohesion. *J. Am. Chem. Soc.* **2004**, *126*, 10230−10231.
(29) He, Y.; Chen, Y.; Liu, H. P.; Ribbe, A. E.; Mao, C. D. Self-Assembly of Hexagonal DNA Two-Dimensional (2D) Arrays. *J. Am. Chem. Soc.* **2005**, *127*, 12202−12203.
(30) Rothemund, P. W. K. Folding DNA to Create Nanoscale Shapes and Patterns. *Nature* **2006**, *440*, 297−302.
(31) Wei, B.; Dai, M. J.; Yin, P. Complex Shapes Self-Assembled from Single-Stranded DNA Tiles. *Nature* **2012**, *485*, 623−626.
(32) Zhang, F.; Jiang, S. X.; Wu, S. Y.; Li, Y. L.; Mao, C. D.; Liu, Y.; Yan, H. Complex Wireframe DNA Origami Nanostructures with Multi-Arm Junction Vertices. *Nat. Nanotechnol.* **2015**, *10*, 779−784.
(33) Wang, P.; Wu, S.; Tian, C.; Yu, G.; Jiang, W.; Wang, G.; Mao, C. Retrosynthetic Analysis-Guided Breaking Tile Symmetry for the Assembly of Complex DNA Nanostructures. *J. Am. Chem. Soc.* **2016**, *138*, 13579−13585.
(34) Han, D. R.; Pal, S.; Nangreave, J.; Deng, Z. T.; Liu, Y.; Yan, H. DNA Origami with Complex Curvatures in Three-Dimensional Space. *Science* **2011**, *332*, 342−346.
(35) Ke, Y. G.; Ong, L. L.; Shih, W. M.; Yin, P. Three-Dimensional Structures Self-Assembled from DNA Bricks. *Science* **2012**, *338*, 1177−1183.
(36) Li, X.; Zhang, C.; Hao, C. H.; Tian, C.; Wang, G. S.; Mao, C. D. DNA Polyhedra with T-Linkage. *ACS Nano* **2012**, *6*, 5138−5142.
(37) Tian, C.; Li, X.; Liu, Z. Y.; Jiang, W.; Wang, G. S.; Mao, C. D. Directed Self-Assembly of DNA Tiles into Complex Nanocages. *Angew. Chem., Int. Ed.* **2014**, *53*, 8041−8044.
(38) Liu, Z.; Tian, C.; Yu, J.; Li, Y.; Jiang, W.; Mao, C. Self-Assembly of Responsive Multilayered DNA Nanocages. *J. Am. Chem. Soc.* **2015**, *137*, 1730−1733.
(39) Li, Y.; Tian, C.; Liu, Z.; Jiang, W.; Mao, C. Structural Transformation: Assembly of an Otherwise Inaccessible DNA Nanocage. *Angew. Chem., Int. Ed.* **2015**, *54*, 5990−5993.
(40) Zhang, G.; Surwade, S. P.; Zhou, F.; Liu, H. DNA Nanostructure Meets Nanofabrication. *Chem. Soc. Rev.* **2013**, *42*, 2488−2496.
(41) Deng, Z. X.; Mao, C. D. Molecular Lithography with DNA Nanostructures. *Angew. Chem., Int. Ed.* **2004**, *43*, 4068−4070.
(42) Jin, Z.; Sun, W.; Ke, Y.; Shih, C. J.; Paulus, G. L. C.; Wang, Q. H.; Mu, B.; Yin, P.; Strano, M. S. Metallized DNA Nanolithography for Encoding and Transferring Spatial Information for Graphene Patterning. *Nat. Commun.* **2013**, *4*, 1663.
(43) Surwade, S. P.; Zhao, S. C.; Liu, H. T. Molecular Lithography through DNA-Mediated Etching and Masking of SiO_2. *J. Am. Chem. Soc.* **2011**, *133*, 11868−11871.
(44) Surwade, S. P.; Zhou, F.; Wei, B.; Sun, W.; Powell, A.; O'Donnell, C.; Yin, P.; Liu, H. T. Nanoscale Growth and Patterning of Inorganic Oxides Using DNA Nanostructure Templates. *J. Am. Chem. Soc.* **2013**, *135*, 6778−6781.
(45) Zhou, F.; Sun, W.; Ricardo, K. B.; Wang, D.; Shen, J.; Yin, P.; Liu, H. Programmably Shaped Carbon Nanostructure from Shape-Conserving Carbonization of DNA. *ACS Nano* **2016**, *10*, 3069−77.
(46) Sun, W.; Boulais, E.; Hakobyan, Y.; Wang, W. L.; Guan, A.; Bathe, M.; Yin, P. Casting Inorganic Structures with DNA Molds. *Science* **2014**, *346*, 1258361.
(47) Pinheiro, A. V.; Han, D. R.; Shih, W. M.; Yan, H. Challenges and Opportunities for Structural DNA Nanotechnology. *Nat. Nanotechnol.* **2011**, *6*, 763−772.
(48) Kershner, R. J.; Bozano, L. D.; Micheel, C. M.; Hung, A. M.; Fornof, A. R.; Cha, J. N.; Rettner, C. T.; Bersani, M.; Frommer, J.; Rothemund, P. W. K.; et al. Placement and Orientation of Individual DNA Shapes on Lithographically Patterned Surfaces. *Nat. Nanotechnol.* **2009**, *4*, 557−561.
(49) Hung, A. M.; Micheel, C. M.; Bozano, L. D.; Osterbur, L. W.; Wallraff, G. M.; Cha, J. N. Large-Area Spatially Ordered Arrays of Gold Nanoparticles Directed by Lithographically Confined DNA Origami. *Nat. Nanotechnol.* **2010**, *5*, 121−126.
(50) Gopinath, A.; Rothemund, P. W. K. Optimized Assembly and Covalent Coupling of Single-Molecule DNA Origami Nanoarrays. *ACS Nano* **2014**, *8*, 12030−12040.
(51) Gopinath, A.; Miyazono, E.; Faraon, A.; Rothemund, P. W. K. Engineering and Mapping Nanocavity Emission *via* Precision Placement of DNA Origami. *Nature* **2016**, *535*, 401−405.
(52) Qu, J. H.; Hou, X. L.; Fan, W. C.; Xi, G. H.; Diao, H. Y.; Liu, X. D. Scalable Lithography from Natural DNA Patterns *via* Polyacrylamide Gel. *Sci. Rep.* **2015**, *5*, 17872.
(53) Li, H.; Wu, J.; Huang, X.; Yin, Z.; Liu, J.; Zhang, H. A Universal, Rapid Method for Clean Transfer of Nanostructures onto Various Substrates. *ACS Nano* **2014**, *8*, 6563−6570.
(54) Ke, Y.; Ong, L. L.; Sun, W.; Song, J.; Dong, M.; Shih, W. M.; Yin, P. DNA Brick Crystals with Prescribed Depths. *Nat. Chem.* **2014**, *6*, 994−1002.
(55) Lee, J.; Kim, S.; Kim, J.; Lee, C. W.; Roh, Y.; Park, S. H. Coverage Control of DNA Crystals Grown by Silica Assistance. *Angew. Chem., Int. Ed.* **2011**, *50*, 9145−9149.
(56) Sun, X. P.; Ko, S. H.; Zhang, C. A.; Ribbe, A. E.; Mao, C. D. Surface-Mediated DNA Self-Assembly. *J. Am. Chem. Soc.* **2009**, *131*, 13248−13249.
(57) Kim, H.; Surwade, S. P.; Powell, A.; O'Donnell, C.; Liu, H. Stability of DNA Origami Nanostructure under Diverse Chemical Environments. *Chem. Mater.* **2014**, *26*, 5265−5273.
(58) Truong, T. T.; Lin, R.; Jeon, S.; Lee, H. H.; Maria, J.; Gaur, A.; Hua, F.; Meinel, I.; Rogers, J. A. Soft Lithography Using Acryloxy Perfluoropolyether Composite Stamps. *Langmuir* **2007**, *23*, 2898−2905.
(59) Li, H. F.; Lin, J. M.; Su, R. G.; Cai, Z. W.; Uchiyama, K. A Polymeric Master Replication Technology for Mass Fabrication of Poly(Dimethylsiloxane) Microfluidic Devices. *Electrophoresis* **2005**, *26*, 1825−1833.
(60) Martínez, E.; Pla-Roca, M.; Samitier, J. Micro/Nanopatterning of Proteins Using a Nanoimprint-Based Contact Printing Technique. In *Nanotechnology in Regenerative Medicine: Methods and Protocols*; Navarro, M., Planell, J. A., Eds.; Humana Press: Totowa, 2012; pp 79−87.
(61) Gates, B. D.; Whitesides, G. M. Replication of Vertical Features Smaller than 2 nm by Soft Lithography. *J. Am. Chem. Soc.* **2003**, *125*, 14986−14987.
(62) Muhlberger, M.; Rohn, M.; Danzberger, J.; Sonntag, E.; Rank, A.; Schumm, L.; Kirchner, R.; Forsich, C.; Gorb, S.; Einwogerer, B.; et al. UV-NIL Fabricated Bio-Inspired Inlays for Injection Molding to Influence the Friction Behavior of Ceramic Surfaces. *Microelectron. Eng.* **2015**, *141*, 140−144.
(63) Xia, Y. N.; McClelland, J. J.; Gupta, R.; Qin, D.; Zhao, X. M.; Sohn, L. L.; Celotta, R. J.; Whitesides, G. M. Replica Molding Using

DOI: 10.1021/acsnano.6b04777
ACS Nano 2017, 11, 227−238

Polymeric Materials: a Practical Step toward Nanomanufacturing. *Adv. Mater.* **1997**, *9*, 147−149.
(64) Zhang, Y.; Lo, C. W.; Taylor, J. A.; Yang, S. Replica Molding of High-Aspect-Ratio Polymeric Nanopillar Arrays with High Fidelity. *Langmuir* **2006**, *22*, 8595−8601.
(65) Gilles, S.; Meier, M.; Prompers, M.; van der Hart, A.; Kugeler, C.; Offenhausser, A.; Mayer, D. UV Nanoimprint Lithography with Rigid Polymer Molds. *Microelectron. Eng.* **2009**, *86*, 661−664.
(66) Pla-Roca, M.; Fernandez, J. G.; Mills, C. A.; Martinez, E.; Samitier, J. Micro/Nanopatterning of Proteins *via* Contact Printing Using High Aspect Ratio PMMA Stamps and Nanoimprint Apparatus. *Langmuir* **2007**, *23*, 8614−8618.
(67) Li, H. W.; Muir, B. V. O.; Fichet, G.; Huck, W. T. S. Nanocontact Printing: a Route to Sub-50-nm-Scale Chemical and Biological Patterning. *Langmuir* **2003**, *19*, 1963−1965.
(68) Schneider, C. A.; Rasband, W. S.; Eliceiri, K. W. NIH Image to ImageJ: 25 Years of Image Analysis. *Nat. Methods* **2012**, *9*, 671−675.

DOI: 10.1021/acsnano.6b04777
ACS Nano 2017, 11, 227−238